Oxidative Degradation of Different Chlorinated Phenoxyalkanoic Acid Herbicides by a Hybrid ZrO$_2$ Gel-Derived Catalyst without Light Irradiation

Filomena Sannino,[†,§] Pasquale Pernice,[‡,§] Luciana Minieri,[‡] Gaia Aurora Camandona,[†] Antonio Aronne,[‡,§] and Domenico Pirozzi*[,‡,§]

[†]Dipartimento di Agraria and [§]Centro Interdipartimentale di Ricerca sulla Risonanza Magnetica Nucleare per l'Ambiente, l'Agro-Alimentare ed i Nuovi Materiali (CERMANU)Università di Napoli Federico II, Via Università 100, 80055 Portici (Napoli), Italy

[‡]Dipartimento di Ingegneria Chimica, dei Materiali e della Produzione Industriale, Università di Napoli Federico II, Piazzale Tecchio 80, 80125 Napoli, Italy

Ⓢ *Supporting Information*

ABSTRACT: The oxidative degradation of 2-methyl-4-chlorophenoxyacetic acid (MCPA), 4-(4-chloro-2-methylphenoxy)butanoic acid (MCPB), 4-chlorophenoxyacetic acid (4-CPA) and 2,4-dichlorophenoxyacetic acid (2,4 D) by ZrO$_2$-acetylacetonate hybrid catalyst (HSGZ) without light irradiation was assessed. The thermal stability of the catalyst was investigated by thermogravimetry, differential thermal analysis, and Fourier transform infrared spectroscopy. For each herbicide, a virtually complete removal in about 3 days without light irradiation at room temperature was achieved. The removal kinetics of the herbicides has been satisfactorily characterized by a double-stage physico-mathematical model, in the hypothesis that a first-order adsorption on HSGZ surface is followed by the herbicide degradation, catalytically driven by HSGZ surface groups. The long-term use of the HSGZ catalyst was assessed by repeated-batch tests. The specific cost for unit-volume removal of herbicide was evaluated by a detailed cost analysis showing that it is comparable with those pertaining to alternative methods.

KEYWORDS: sol−gel, zirconium oxide, hybrid catalyst, chlorinated phenoxyalkanoic acid herbicides, oxidative degradation
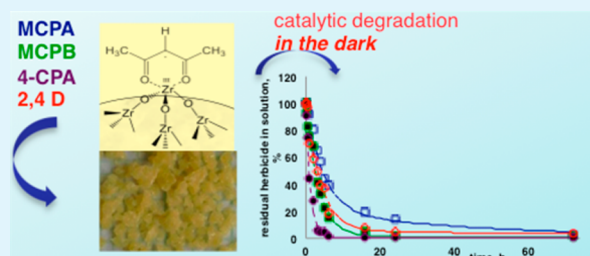
1. INTRODUCTION

Chlorinated phenoxyalkanoic acid herbicides are largely distributed in the environment because of their widespread use for weed control in agricultural crops. Because of their chemical stability, resistance to biodegradation, and sufficient water solubility, these compounds can either reach the groundwaters or be washed away to the surface water bodies.

They are considered to be harmful to human health because of the potential mutagenicity and toxicity, and are listed by the U.S. Environmental Protection Agency (EPA) as priority pollutants.[1] For this reason, the risk of environmental pollution of soil and waters must be considered and the development of new remediation technologies appears to be of primary importance.

Many research efforts have been devoted to developing methods for the elimination of such recalcitrant pollutants from soils and waters by means of biological and chemical-physical methods.

Biodegradation has received the greatest attention because is efficient and relatively cheap; however, it is susceptible to toxic compounds that inactivate the waste degrading microorganisms. Among many processes proposed,[2−6] sorption and degradation are the two most important for the herbicide

remediation. In several instances, a clear connection has been observed between them.

For example, in the biological remediation of soils, it is commonly accepted that sorbed herbicides are less accessible to soil microorganisms, and consequently sorption limits the herbicide degradation.[7−9] The opposite situation occurs when an inorganic catalyst promotes the degradation mechanism. In this case, herbicide sorption is required for the degradation to be carried out.

To produce an effective removal of herbicides, adsorbents have to satisfy different conditions:

(i) to selectively adsorb herbicides, limiting the occupation of adsorption sites with other compounds contained in the wastewaters;

(ii) to have a high sorption capacity for the herbicides;

(iii) to be easily regenerated by cheap and simple procedures; this means that the interaction with the adsorbent has to be weak enough to be reversible;

(iv) in alternative or in addition to condition iii, adsorption should be accompanied by chemical transformation of herbicides in simpler products, having much lower toxicity, and lower interactions with the sorbent materials to enable its easier regeneration.

Among the technologies that involve the use of inorganic catalysts, advanced oxidation processes (AOPs) have been widely used for the wastewaters treatment over the last few decades.[10] In particular, the combined use of oxidants (e.g., ozone, H_2O_2, UV radiation) and photocatalysts (e.g., TiO_2 and V_2O_5) have received the most attention. TiO_2 is the dominant system in the environmental applications as it is efficient to decompose pollutants under irradiation by ultraviolet light (band gap around 3.2 eV). But its low quantum efficiency, due to inefficient capture of sunlight that contains prevalently visible and near-infrared radiation, represents a strong limitation to applications. To overcome this drawback, different approaches have been explored that aim to reduce the optical band gap between conduction band (CB) and valence band (VB) of the semiconducting oxide, such as doping with transition metal ions,[11,12] dyes, noble metals particles, and narrow band gap semiconductors,[13] or by surface modification with charge-transfer complexes.[14]

ZrO_2, another semiconducting oxide, has found only few applications in photocatalysis because of its larger band gap (about 5.0 eV), an energy corresponding to a negligible fraction of the sunlight, even if, recently, Ce-ZrO_2 heterostructures have showed photosensitivity to visible light as consequence of the formation of intraband gap between the CB and the VB of the oxide because of Ce 4f empty states.[15]

Recently, we have synthesized hybrid and biohybrid gel-derived ZrO_2-based materials that have shown very high remediation activity toward organic pollutants from aqueous solution, such as phenanthrene (PHE)[16] and the herbicide 4-chloro-2-methylphenoxyacetic acid.[17,18] In particular, we have demonstrated that this ZrO_2-acetylacetonate hybrid material (HSGZ) exhibits its intrinsic catalytic activity toward the oxidative degradation of PHE acting as radicals initiator without any light irradiation at 30 °C. Free radicals were formed by an intramolecular acac-to-metal electron transfer mechanism giving on the solid surface the equilibrium between Zr(IV)-acac and Zr(III)-acac● complexes, from which in the presence of molecular O_2 reactive oxygen species are produced.[16] Therefore, this material allows extending the frontiers of ZrO_2 application to pollutants degradation as its functionality does not require any activation procedure neither thermal nor light.

In this paper, the HSGZ catalytic activity toward the oxidative degradation of four different phenoxy herbicides have been explored with special reference to evaluation of their degradation kinetics. Moreover, a systematic characterization of the HSGZ is reported aimed to study the thermal stability of the Zr-acac complexes that represents the structural feature responsible of the catalytic activity. Finally, in view of the real application of this material, a cost analysis for a batch reactor is also reported.

The herbicides investigated, classified as potential groundwater contaminants by U.S. EPA, are 4-chloro-2-methylphenoxyacetic acid (MCPA), 4-chlorophenoxyacetic acid (4-CPA), and 2,4-dichlorophenoxyacetic acid (2,4-D) belonging to the phenoxyacetic group, and 4-(4-chloro-2-methylphenoxy) butanoic acid (MCPB), a phenoxybutyric herbicide.

2. MATERIALS AND METHODS

2.1. Materials. 4-Chloro-2-methylphenoxyacetic acid (MCPA), 4-chlorophenoxyacetic acid (4-CPA), 2,4-dichlorophenoxyacetic acid (2,4 D), and 4-(4-chloro-2-methylphenoxy)butanoic acid (MCPB) were purchased from Sigma-Aldrich Chemical Co. (Poole, Dorset, UK; 99.0% purity). The structural formula of each herbicide is reported in Figure S1 of Supporting Information. All solvents were of HPLC grade (Carlo Erba, Milan, Italy) and were used without further purification. Zirconium(IV) propoxide (70 wt % in 1-propanol), acetylaceton (>99%), and 1-propanol (>99.80%) were provided by Sigma-Aldrich.

2.2. Sol−Gel Synthesis. The HSGZ matrix was prepared according to the procedure reported elsewhere.[18] A solution containing 10 mL of zirconium(IV) propoxide (70 wt % in 1-propanol) (22.6 mmol), 1.5 mL of acetylacetone (99+%) (14.6 mmol), and 3.0 mL of 1-propanol (99.80+%) (39.9 mmol) was prepared and stirred at room temperature for a few minutes. A second solution containing 3.0 mL of distilled water (166 mmol) and 5.5 mL of 1-propanol (73.2 mmol) was added to the first one. The solution obtained was vigorously stirred until the gelation that occurred in about 20 min at room temperature. A homogeneous slightly yellow colored gel was obtained. The gel was left at room temperature for 2 days and then dried at 30 °C, giving a porous amorphous xerogel (HSGZ). Powders of granulometric distribution ranging from 63 to 90 μm were selected to perform the kinetic tests.

2.3. Thermal and Structural Characterization. To study the reactions occurring during xerogels heating, we carried out thermogravimetric (TG) and differential thermal (DTA) analyses, using a TA Instruments SDT Q 600. The TG and DTA tests were performed keeping 20−25 mg of xerogel under nitrogen atmosphere, varying the temperature from 20 to 1000 °C. A heating rate of 10 °C min^{-1} was adopted.

The amorphous nature of the dried gels as well as the nature of the crystallizing phases were ascertained by X-ray diffraction with a Philips X'PERT−PRO diffractometer by using monochromatized CuKα radiation (40 mA, 40 kV) with a step width of 0.013° 2θ.

The structure of the HSGZ matrix, as well as its structural evolution during the heating, was studied by Fourier transform infrared (FTIR) spectroscopy.

FTIR spectra of dried and heat-treated gel samples were carried out at room temperature by a Nicolet system, Nexus model, equipped with a DTGS KBr (deuterated triglycine sulfate with potassium bromide windows) detector. The absorption spectra were recorded in the 4000−400 cm^{-1} range with a spectral resolution of 2 cm^{-1} on samples diluted in KBr. The spectrum of each sample represents an average of 64 scans, which were corrected for the spectrum of the blank KBr.

Moreover, FTIR spectrum of HSGZ after repeated batch tests in the presence of 0.2 mmol L^{-1} of MCPB solution was recorded at room temperature.

2.4. Analytical Determination of MCPA, 4-CPA, 2,4-D and MCPB. All the herbicides were analyzed with an Agilent 1200 Series HPLC apparatus (Wilmington U.S.), equipped with a DAD and a ChemStation Agilent Software. A Macharey-Nagel Nucleosil 100−5 C18 column (stainless steel 250 × 4 mm) was utilized.

As regards MCPA, the mobile phase composed of a binary system of 50:50 acetonitrile: phosphate buffer (0.1%, pH 2.5) was pumped at 1 mL min^{-1} flow in isocratic mode. The detector was set at 225 nm. MCPB was analyzed using the same conditions, except of the eluent system that consisted of a binary system of 60:40 acetonitrile: phosphate buffer (0.1%, pH 2.5).

For 2,4-D and 4-CPA, the mobile phase composed of a binary system of 40:60 acetonitrile: phosphate buffer (0.1%, pH 2.5) was pumped at 1 mL min^{-1} flow in isocratic mode. The detector was set at 283 nm. For all herbicides chosen the injection volume was 20 μL.

The quantitative determination was performed using a calibration curve for each herbicide investigated. The following concentration ranges were adopted: 0.0002−0.9 mmol L^{-1}, 0.0001−0.2 mmol L^{-1}, 0.0002−2.7 mmol L^{-1}, and 0.0002−2.0 mmol L^{-1}, for MCPA, MCPB, 4-CPA and 2,4-D, respectively.

2.5. Removal Tests of MCPA, 4-CPA, 2,4-D, and MCPB by HSGZ Matrix. A stock solution of each herbicide was prepared by dissolving in 500 mL of Milli-Q ultrapure water the following amounts: 100 mg of MCPA (final concentration 0.9 mmol L^{-1}); 22 mg of MCPB (final concentration 0.2 mmol L^{-1}); 250 mg of 4-CPA (final concentration 2.7 mmol L^{-1}) and 250 mg of 2,4-D (final concentration 2.0 mmol L^{-1}). The solutions obtained were subsequently kept refrigerated.

All the experiments were carried out in batch conditions in the dark, in a thermostatic rotary shaker at 30 °C. Blanks of each herbicide in aqueous solution were analyzed in order to check the pesticide stability and the possible sorption to vials. After incubation, the samples were centrifuged at 7000 rpm for 20 min and the supernatants were analyzed as above-reported.

Kinetic experiments were performed incubating 1 mg of HSGZ matrix with 1 mL of each herbicide (solid/liquid ratio $R = 1.0$) at 0.2 mmol L^{-1} concentration for different incubation times (0.25, 0.5, 1.0, 2.0, 3.0, 4.0, 5.0, 6.0, 16, 24, 72 h) at 30 °C.

In order to clarify the effect of the herbicide concentration, we carried out kinetic tests, as above-reported, adopting for each herbicide concentration values close to solubility limits. The experiments were conducted at $R = 1.0$ using solutions at 0.9, 0.2, 2.7, and 2.0 mmol L^{-1} of MCPA, MCPB, 4-CPA, and 2,4-D, respectively, at 30 °C.

With the purpose to investigate the effect of HSGZ matrix amount, kinetic tests of MCPA removal were performed at 0.2 mmol L^{-1} concentration and at $R = 1.0$, 2.0 (obtained by adding 4 mg of matrix in 2.0 mL of final volume), and 5.0 (obtained by adding 10 mg of matrix in 2.0 mL of final volume).

Finally, the long-term applicability of the MCPB-removal system was verified by carrying out repeated batch tests. After each batch test, the liquid phase was removed and replaced by an equal volume of MCPB solution at the initial concentration of 0.2 mmol L^{-1}. To investigate the stability of the catalyst, we recorded FTIR spectrum of HSGZ before and after repeated batch tests at room temperature.

2.6. Kinetic Models. The removal kinetics of the four herbicides on the HSGZ were elaborated considering three different kinetic models: a pseudo-first-order,[19] a pseudo-second-order,[19] and a physico-mathematical.[18] The kinetic model to be used for the experimental data modeling was selected on the basis of the highest correlation coefficient r^2 as described in more detail in the paragraph S1 and Table S1 (Supporting Information).

2.7. Analysis of the Data. All the experiments were carried out in triplicate and the relative standard deviation was lower than 4%.

3. RESULTS AND DISCUSSION

3.1. Thermal and Structural Characterization of HSGZ Xerogel. TG/DTA curves of HSGZ xerogel having a granulometric distribution ranging from 63 to 90 μm, recorded in nitrogen at 10 °C min^{-1}, are reported in Figure 1 together with the corresponding room temperature FTIR spectra.

With respect to the TG/DTA curves of lyophilized HSGZ xerogel[18] these curves display a few differences: the overall weight loss that appears slightly higher (35 wt %); on the TG curve only three distinct inflection points are observed in the range 25−400 °C (∼58 °C, ∼201 °C, and ∼332 °C) corresponding to three DTA endothermic peaks, the former two being overlapped; two unresolved DTA exothermic peaks at about 455 and 515 °C occur in the temperature range in which the crystallization of zirconia takes place and in the corresponding TG curve an additional inflection point is seen (∼519 °C) even if it related to a very small weight loss, less than 2 wt %. On the contrary, any detectable difference is seen by comparing the FTIR spectra of lyophilized[18] and dried HSGZ xerogels (Figure 1) except for the splitting (Δ) between the asymmetric ($\nu_{asyC=O}$) and symmetric ($\nu_{symC=O}$) stretching of C=O bonds of the carboxylate groups, that results slightly higher Δ = 140 cm^{-1}. Nevertheless, this Δ value lies in the 50−
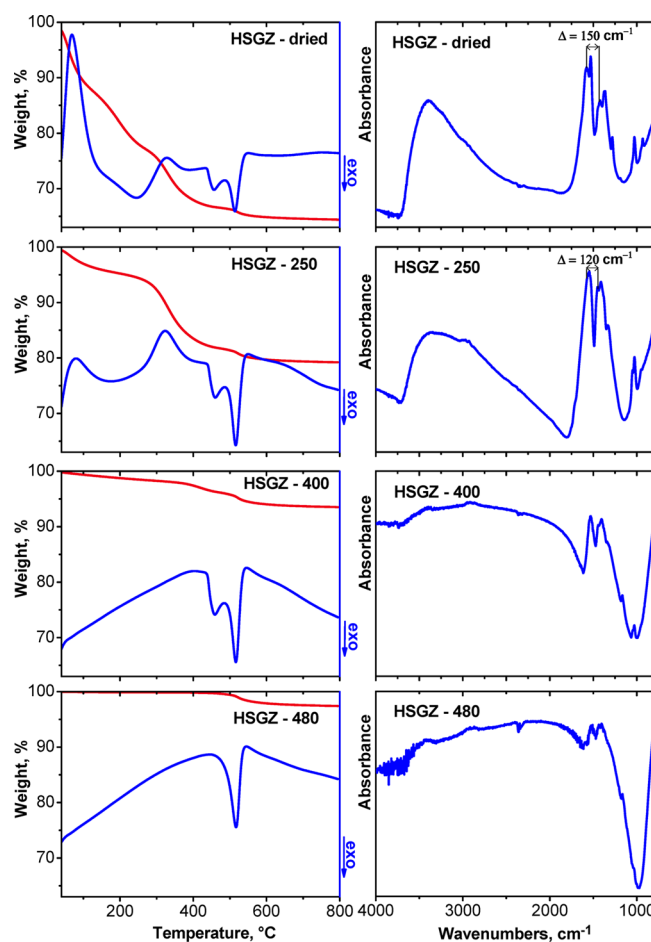

Figure 1. On the left: TG/DTA curves, recorded in nitrogen at 10 °C/min, of HSGZ as dried (HSGZ-dried) and heated up to 250 (HSGZ-250), 400 (HSGZ-400), and 480 °C (HSGZ-480). On the right the corresponding room-temperature FTIR spectra.

150 cm^{-1} range attesting the existence of a bidentate interaction between the acac and Zr^{4+} in the Zr-acac complexes.[20]

To identify the nature of each DTA peak, different heat-treated samples were prepared, by heating at 10 °C min^{-1} up to the required temperature and then quenching. Hereafter the samples will be noted as the acronym HSGZ followed by heat-treatment temperature, i.e., HSGZ-250, HSGZ-400, HSGZ-480.

The DTA curve of HSGZ-250 (see Figure 1) still exhibits a residual and low intensity endothermic peak at low temperature (∼80 °C), which is related to the loss of water adsorbed during the cooling at room temperature because of the porous nature of HSGZ, whereas the DTA endopeak at about 330 °C as well as the two DTA exopeaks remain unchanged. Also the corresponding FTIR spectrum (see Figure 1) remains almost unchanged except for the Δ value that becomes lower (Δ = 120 cm^{-1}) even if it is still in the 50−150 cm^{-1} range indicating the presence of Zr-acac complexes. Therefore, by heating up to 250 °C the evaporation of water and alcohol physically trapped in the gels as well as the pyrolysis of organics originated during the gelation and during the heating take place, but acac ligands are still retained. The FTIR spectrum of HSGZ-400 (see Figure 1) does not exhibit the characteristic absorption bands related to $\nu_{asyC=O}$ and $\nu_{symC=O}$. It shows two main absorption bands at about 1500 cm^{-1} (ν_{C-C}) and 1440 cm^{-1} (δ_{CH2}), that are related

258

dx.doi.org/10.1021/am506031e | *ACS Appl. Mater. Interfaces* 2015, 7, 256−263

to residual organics, allowing to state the lack of Zr-acac complexes at this stage, and consequently, to assign the DTA endopeak at about 330 °C, seen in the DTA curves of HSGZ and HSGZ-250, to the loss of the acac ligands. The high temperature of this peak indicates that acac ligands are strongly bonded to the solid matrix giving a highly stable hybrid material.

To identify the nature of two DTA exopeaks seen in the DTA curve of HSGZ-400 (see Figure 1), HSGZ-400 was used to prepare two samples by heating at 10 °C/min up to 480 °C (just up the maximum of the first DTA exopeak, HSGZ-400/480) and 550 °C (after the end of the second DTA exopeak, HSGZ-400/550) and then quenched. The corresponding XRD profiles are shown in Figure 2 where the pattern of HSGZ-400
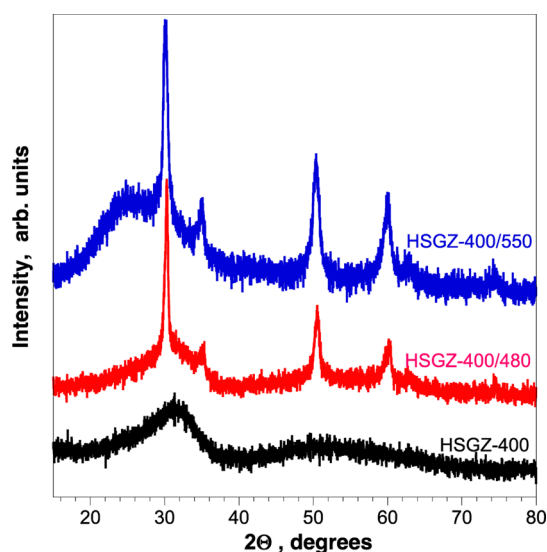

Figure 2. XRD patterns: dried gel heated up to 400 °C and then quenched (HSGZ-400); this sample heated up to 480 °C (HSGZ-400/480) and up to 550 °C (HSGZ-400/550).

is also reported. The latter XRD pattern shows that HSGZ keeps its amorphous nature up to 400 °C. The formation of ZrO_2 nanocrystals of the tetragonal polymorph, T-ZrO_2, (JCPDS card 50−1089) starts to occur at the first DTA exopeak. The distinction between tetragonal and cubic phase is not an easy task on account of the overlapping reflections; nevertheless, we are confident of the above-reported assignment given the lack of (040) reflection at $2\theta = 73.98°$ characteristic of the cubic polymorphous and the presence of the peak at $2\theta = 74.58°$ detectable for the tetragonal polymorph.[21]

The shape and the position of DTA crystallization peak differ from the ones previously reported for a zirconia gel-derived material prepared using a different Zr/acetylacetone molar ratio[21] so confirming that, when the crystallization starts from an amorphous sol−gel matrix, both the temperature and the rate of crystallization are strongly influenced by solution chemistry. On the other hand, differences were also found with respect to the lyophilized HSGZ xerogel[20] indicating that the surface specific area of the sample also influences the crystallization. It should be underlined that what said refers to nonisothermal crystallization, that is occurring during a DTA run at 10 °C min⁻¹.

Comparing the XRD profiles of HSGZ-400/480 and HGSZ-400/550 no differences are seen, in both samples only T-ZrO_2

nanocrystals are formed (see Figure 2). On the contrary, the shape of the amorphous halo changes in the 20−30° 2θ range, exhibiting a great increase for the HSGZ-400/550 in the corresponding of the highest monocline peak. This result with TG/DTA curves of HSGZ-480 (see Figure 1) showing a single DTA exopeak and a corresponding inflection point (∼519 °C) on TG curve allow to relate this thermal effect mainly to a modification of the HSGZ amorphous matrix that is partially overlapped to T-ZrO_2 crystallization.

During the nonisothermal devitrification, the growth of a crystalline phase, different from the thermodynamically stable one, has been often observed; namely, it can be said that during a DTA run, the phase that grows faster will be obtained, regardless of the thermodynamic stability and chemical composition.[22] The initial formation of the metastable tetragonal phase occurring from the nonisothermal crystallization of zirconia dried gel can be explained on the basis of its structural similarity with the sol−gel matrix.[21] Its formation is driven and controlled by kinetic aspects. When the crystallization starts from a preheated sample, such as HSGZ-400, the transformation involves mainly the residual amorphous phase and the thermodynamic aspects begin to prevail, facilitating the transformation toward the stable monoclinic phase.

3.2. Modeling of Removal Kinetics. The kinetics of removal of the four herbicides in the presence of HSGZ is shown in Figure 3. For the sake of comparison, the initial concentration (C_0) of all the four herbicides has been set at 0.2 mmol L⁻¹, and the solid/liquid ratio (R) is 1.0.
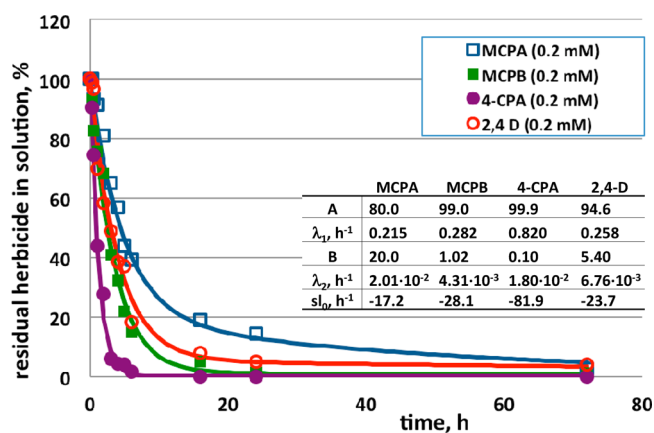

Figure 3. Kinetics of herbicide removal at 30 °C, in the presence of HSGZ matrix. Herbicides: MCPA (□), MCPB (■), 4-CPA (●), 2,4-D (○). $C_0 = 0.2$ mmol L⁻¹, $R = 1$. The interpolation curves have been obtained using mathematical model 2. The estimated parameters are reported in the box.

The experimental data demonstrate that an almost complete removal of the herbicides can be achieved in about 3 days. As the concentration−time profiles could not be satisfactorily described by a pseudo-first-order kinetic model[19] or a pseudo-second-order kinetic model,[19] (both models showed a low correlation coefficient r^2), an alternative physico-mathematical model, previously developed for MCPA removal[18] was used to elaborate the data. Briefly, the model is based on the hypothesis that reversible, first-order adsorption on HSGZ surface is the first stage of the herbicide removal as usually occurs in heterogeneous catalysis. The subsequent reaction of herbicides,

catalytically driven by HSGZ surface groups, yields degradation products, according to the scheme

$$C_{sol} \underset{k_{-1}}{\overset{k_1}{\rightleftharpoons}} C_{ads} \overset{k_2}{\rightarrow} P \tag{1}$$

where C_{ads} is the concentration of adsorbed herbicide, P indicates the degradation products, k_1 and k_{-1} are the direct and inverse first-order kinetic constants of the herbicide sorption, and k_2 is the first-order kinetic constants of the herbicide degradation.

The mass balances applied to the chemical species involved in model 1 yield concentration−time profiles describing the herbicide removal by double-exponential curves[18]

$$C_{sol}(t) = Ae^{-\lambda_1 t} + Be^{-\lambda_2 t} \tag{2}$$

where C_{sol} is the herbicide concentration in the liquid phase (mmol L^{-1}), and t the time (h).

Mathematical model 2, previously tested only for MCPA removal, could satisfactorily be used to interpolate the experimental data. The interpolating curves are dashed in Figure 3, together with the estimated values of the model parameters.

In order to elaborate the experimental data, model 2 was used to evaluate the initial slope of the concentration profiles, i.e., the initial removal rate of herbicide (also reported in Figure 3)

$$sl_o = \left. \frac{dC_{sol}(t)}{dt} \right|_{t=0} = -\lambda_1 A - \lambda_2 B \tag{3}$$

We also observed that when the hypothesis $\lambda_1 \gg \lambda_2$ can be made (as for the curves in Figure 3), the first exponential term in expression 2 decays much faster than the second exponential term. Consequently, the final part of each concentration profiles in Figure 3 can be described by the second exponential term. Physically, the decay of the first exponential term corresponds to the achievement of a pseudostationary condition in the first stage of mechanism 1, i.e., the sorption on HSGZ. Once this condition is achieved, further changes in the concentration profiles of herbicides are much slower, as they reflect the kinetics of herbicide degradation (second stage in mechanism 1), that is described by the second exponential term in the expression 2. Therefore, when $\lambda_1 \gg \lambda_2$, it is possible to assume the parameter λ_2 to coincide with the first-order kinetic constant of the herbicide degradation (k_2). On the other hand, the pre-exponential term B can be seen as a measurement of the herbicide amount that remains in liquid phase once the pseudostationary condition is reached.

Under the experimental conditions adopted to obtain the curves in Figure 3, the initial removal rate of 4-CPA (also reported in Figure 3) was significantly faster as compared to those observed when testing the other herbicides. This was because of the higher sorption rate, as the degradation rate for 4-CPA was not faster than those pertaining to other herbicides.

The values of B were close to zero when using MCPB and 4-CPA, indicating that most of herbicide was removed before the pseudostationary condition was reached. In the tests with 2,4-D and with MCPA, higher values of B were obtained. This indicates that the HSGZ was not able to fully adsorb the herbicide, and the total solute removal was obtained slowly, as the progressive degradation of the adsorbed herbicide shifted the sorption equilibrium. However, the fastest degradation rate was observed in the presence of MCPA.

To clarify the effect of the herbicide concentration, we carried out removal tests adopting for each herbicide C_0 values close to solubility limits, as shown in Figure 4.
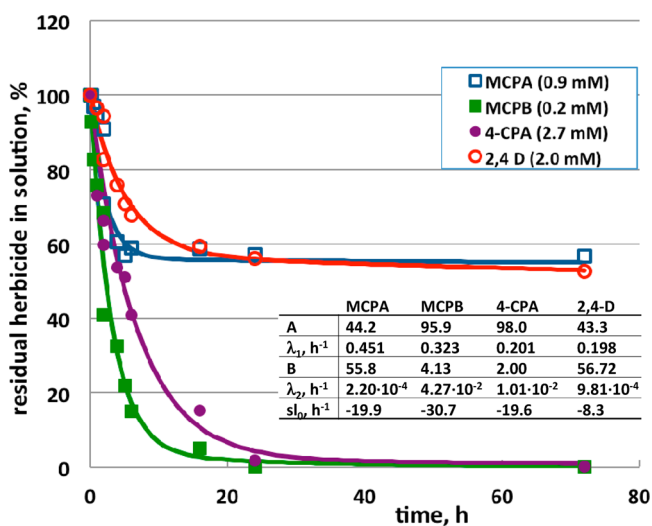

Figure 4. Kinetics of herbicide removal at 30 °C, in the presence of HSGZ matrix. Herbicides: MCPA (□), MCPB (■), 4-CPA (●), 2,4-D (○). Values of C_0 (mmol L^{-1}) adopted for each herbicide: 0.9 (MCPA), 0.2 (MCPB), 2.7 (4-CPA), 2.0 (2,4-D). R = 1. The interpolation curves have been obtained using mathematical model 2. The estimated parameters are reported in the box.

	MCPA	MCPB	4-CPA	2,4-D
A	44.2	95.9	98.0	43.3
λ_1, h^{-1}	0.451	0.323	0.201	0.198
B	55.8	4.13	2.00	56.72
λ_2, h^{-1}	$2.20 \cdot 10^{-4}$	$4.27 \cdot 10^{-2}$	$1.01 \cdot 10^{-2}$	$9.81 \cdot 10^{-4}$
sl_0, h^{-1}	-19.9	-30.7	-19.6	-8.3

When working at higher herbicide concentrations, higher values of B were obtained for all the herbicides tested, due to the reduction of herbicide fraction removed during the initial sorption. In particular, when using MCPA and 2,4-D, about 50% of herbicide was still in solution once the pseudostationary condition was achieved. In all cases, the rate of degradation was slower as the initial C_0 concentration increased.

The effect of the HSGZ concentration (R) is shown in Figure 5, with reference to the MCPA degradation.

The experimental data demonstrate that, as R increases, the initial rate of the MCPA removal is faster. Increasing the concentration of catalyst (R), a lower amount of residual herbicide still dissolved in solution is found once the pseudostationary condition is achieved, as shown by the decrease of the parameter B.

Similar trends were observed when changing the catalyst concentration in the presence of other herbicides. The results obtained with 2,4-D and 4-CPA are summarized in Table 1.

Again, increases in the zirconia concentration (R) produced higher values of the initial rate of the MCPA removal, as well as lower values of the parameter B.

When adopting MCPA concentration not above 0.2 mmol L^{-1}, a complete herbicide removal was obtained in a treatment time of 24−72 h. On the basis of these results, it can be observed that the kinetics of herbicide removal by sorption/degradation mechanism using HSGZ is comparable to that obtained by photodegradation,[23−25] and in any case they were much faster in comparison to ones achieved by bioaugmentation.[26,27]

In the last few decades advanced oxidation processes (AOPs) have been widely used for organic pollutants degradation. Particularly, AOPs combining oxidants (e.g., ozone and H_2O_2), UV radiation and catalysts (e.g., TiO_2 and V_2O_5) have received most of the attention.[28] For example, Gurol and Vatistas[29]
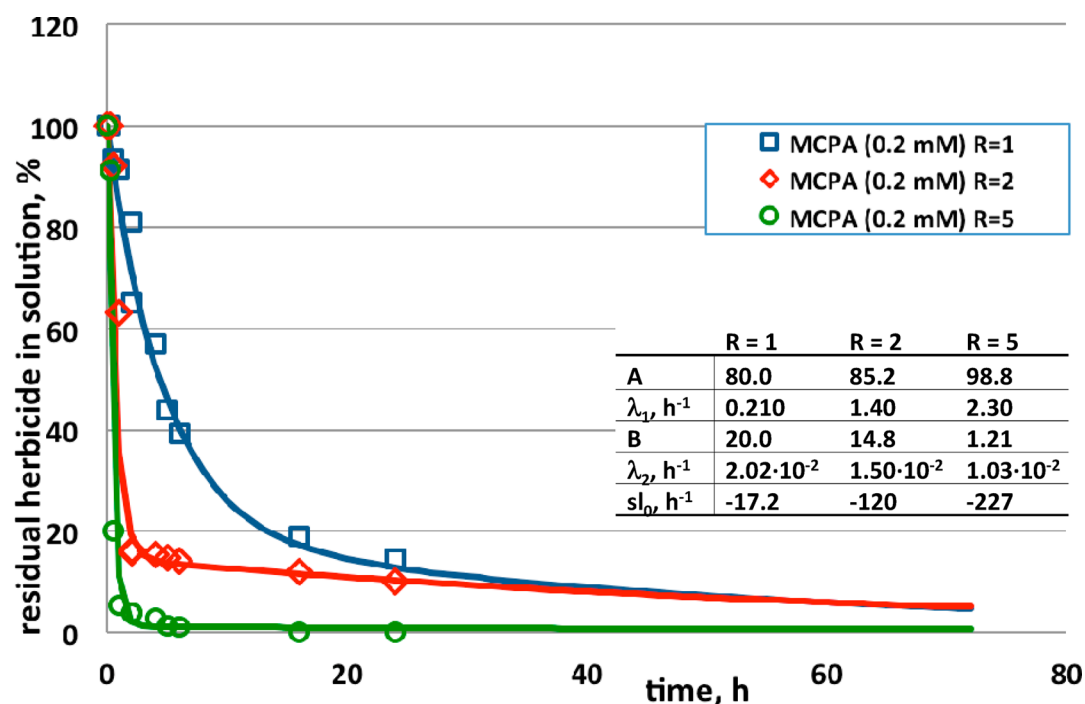
Figure 5. Kinetics of MCPA removal at 30 °C, in the presence of HSGZ matrix. C_0 = 0.2 mmol L^{-1}. Values of R: 1.0 ($\square$), 2.0 ($\Diamond$), 5.0 ($\bigcirc$). The interpolation curves have been obtained using mathematical model 2. The estimated parameters are reported in the box.

Table 1. Values of Parameters of the Physico-Mathematical Model Obtained from the Removal Test of 2,4-D[a] and 4-CPA[a] at 30 °C, in the Presence of HSGZ Matrix

	2,4-D			4-CPA		
	R = 1.0	R = 2.0	R = 5.0	R = 1.0	R = 2.0	R = 5.0
A	94.6	109	116	99.9	114	117
λ_1 (h^{-1})	0.250	0.271	0.282	0.821	0.625	0.640
B	5.40	3.65	2.98	0.110	0.082	0.071
λ_2 (h^{-1})	6.76×10^{-3}	2.48×10^{-3}	1.05×10^{-3}	1.80×10^{-2}	1.11×10^{-2}	7.84×10^{-3}
sl_0 (h^{-1})	−23.7	−98.0	−201	−81.9	−340	−844

[a]C_0 = 0.2 mmol L^{-1}.

treated a mixture of phenol, *p*-cresol, 2,3-xylenol, and catechol with ozone, UV light, and a combination of them (photolytic ozonation). They observed that more than 95% of the total organic carbon was removed in the combined treatment (ozone and UV light). Li et al.,[30] demonstrated that phenol was rapidly oxidized by a Ti/SnO$_2$−Sb anode, and its concentration drastically decreased (total removal) after electrolysis carried out for 5 h. Ugurlu and Karaoglu[31] showed that more than 90% phenol was degraded within 24h by using UV/H$_2$O$_2$/TiO$_2$/Sepiolite. Other authors[32] demonstrated the 4-CPA degradation by advanced electrochemical oxidation processes such as electro-Fenton and photoelectron-Fenton with UV-light, using an undivided cell containing a Pt anode. In these conditions, the main oxidant was hydroxyl radical produced from Fenton's reaction between Fe^{2+} added to the medium and H$_2$O$_2$ electrogenerated from an O$_2$-diffusion cathode. Solutions of 4-CPA at <400 ppm concentration were completely mineralized at low current by photoelectron-Fenton, whereas electro-Fenton caused approximately 80% of mineralization.

3.3. Long-Term Application of HSGZ Matrix. To evaluate the suitability of the HSGZ matrix for commercial application, we tested the long-term performance of the catalyst by carrying out repeated batch cycles of MCPB removal. Each

batch sorption cycle was carried out for 1 h at 30 °C and R = 10, restoring the initial concentration of MCPB (0.2 mmol L^{-1}) after each test. In Figure 6, no significant change is seen in the FTIR spectrum of HSGZ after 6 batches indicating the stability of the catalyst. Moreover only a moderate decrease of the fractional MCPB removal from the first test (85%) to the second (80%) is revealed by the data in the inset. Nevertheless, the removal efficiency remains virtually constant in the following 5 tests. On the basis of these results, it can be envisaged that a long-term use of the HSGZ matrix is possible.

3.4. COST ANALYSIS

A cost analysis was carried out for the removal of MCPA by HSGZ in a batch reactor (see the Supporting Information for details). A volume of 1×10^5 L/day of the herbicide solution at the initial concentration C_0= 10^{-3} g L^{-1} was assumed as basis for the estimated costs. The plant specifications are reported in Table 2a. The target of the process was to obtain a 95% reduction of the herbicide concentration (i.e., to obtain a final herbicide concentration C_{fin}= 5×10^{-2} g L^{-1}).

To carry out the analysis, the capital investments, the direct annual costs and the indirect annual costs were assessed. The complete procedure is detailed in the Supporting Information.
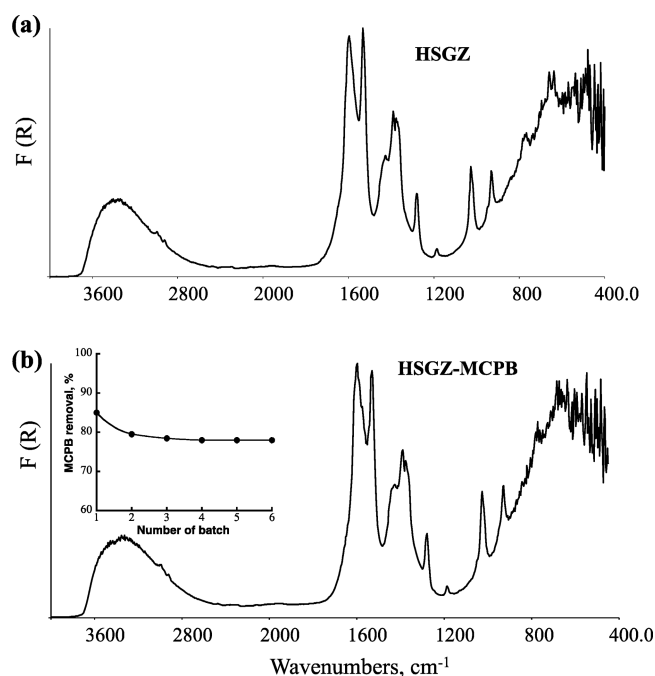
Figure 6. FTIR spectra recorded at room temperature. (a) HSGZ matrix; (b) HSGZ matrix after six repeated batch tests with 0.2 mmol L^{-1} of MCPB solution. In the inset of the b, repeated batch tests are reported.

Table 2. Specifications and Operating Costs of a Plant of MCPA Removal by HSGZ

(a) Plant Specifications	
initial conc. of herbicide	1×10^{-3} g L^{-1}
final conc. of herbicide	5×10^{-5} g L^{-1}
fraction of herbicide removed	95%
volume of liquid processed in a day	1×10^{5} L/day
Volume of the reactor	8333 L
concentration of HSGZ	1 g L^{-1}
lifetime of HSGZ	5 cycles
operation time for a cycle	1.5 h
dead time	0.5 h
(b) Operating Costs	
capital investment	$155,033
direct annual costs	$124,392
indirect annual costs	$27,906
total annual costs	$152,298
cost for unit volume	$4.17 m^{-3}

The operating costs of a plant for MCPA removal by HSGZ are reported in Table 2b. The results show that total annual costs are dominated by the direct annual costs, that are mainly made of the cost of the HSGZ preparation, with a significant contribution of the labor and electricity costs.

The specific cost for unit volume of herbicide solution ($4.17 m^{-3}) is comparable with the value estimated for the TiO_2-based catalytic photooxidation.[33] Nevertheless, this cost can be significantly reduced (at least 1 order of magnitude) and made economically competitive with the current treatment methods, for different reasons:

- The formulation of the HSGZ, as well as the operating conditions, can be further on optimized to improve the herbicide-removal kinetics and the lifetime of the material.

- As the spent HSGZ partially keeps its catalytic activity after the operating cycle, its long-term storage is likely to lead to the complete degradation of the residual herbicide in the internal pores. In this case, no disposal of the material is required and the disposal costs are close to zero.

In addition, it should be taken into account that the experimental conditions adopted in this work, and consequentially the conditions considered for the cost analysis, refer to relatively high values of herbicide concentration. If the treatment is to be carried out for the purification of drinkable water, the amounts of herbicide to remove will be much lower, and will require lower amounts of HSGZ material. This will significantly affect the total annual costs, as the latter have been shown to be mainly made of the cost of HSGZ, though perspectives for a process improvement and the eventual reduction of the costs can be envisaged.

4. CONCLUSION

The oxidative degradation of different chlorinated phenoxyalkanoic acid herbicides, MCPA, 2,4-D, 4-CPA, and MCPB by ZrO_2-acetylacetonate hybrid catalyst (HSGZ) without light irradiation was assessed with special reference to evaluation of their degradation kinetics. A virtually complete removal in about 3 days at room temperature was achieved for the four herbicides. This result is comparable to those usually obtained by photo-oxidation.[24,31] The cost for unit volume of herbicide solution was comparable with the value estimated for the photo-oxidation treatments, as well.

The systematic characterization of HSGZ investigated by thermogravimetry, differential thermal analysis, and Fourier transform infrared spectroscopy indicated that it is a highly stable hybrid material. Finally, a long-term application of the HSGZ catalyst tested by repeated-batch tests was achieved.

■ ASSOCIATED CONTENT

ⓢ Supporting Information

Selection of the kinetic model used for the experimental data modeling; cost analysis for the removal of MCPA by HSGZ in a batch reactor; structural formulas of the four herbicides. This material is available free of charge via the Internet at http://pubs.acs.org/.

■ AUTHOR INFORMATION

Corresponding Author
*E-mail: dpirozzi@unina.it. Tel.: +39 0817682274.

Notes
The authors declare no competing financial interest.

■ REFERENCES

(1) Walker, M.; Lawrence, H. *EPA's Pesticide Fact Sheet Database*; Lewis Publishers: Chelsea, MI, 1992.

(2) Werner, D.; Garratt, J. A.; Pigott, G. Sorption of 2,4-D and Other Phenoxy Herbicides to Soil, Organic Matter, and Minerals. *J. Soils Sediments* **2013**, *13*, 129−139.

(3) Bahnemann, W.; Muneer, M.; Haque, M. M. Titanium Dioxide-Mediated Photocatalysed Degradation of Few Selected Organic Pollutants in Aqueous Suspensions. *Catal. Today* **2007**, *124*, 133−148.

(4) Singh, H. K.; Saquib, M.; Haque, M. M.; Muneer, M. Heterogenous Photocatalysed Degradation of 4-Chlorophenoxyacetic Acid in Aqueous Suspensions. *J. Hazard. Mater.* **2007**, *142*, 374−380.

(5) Olaniran, A. O.; Igbinosa, E. O. Chlorophenols and Other Related Derivatives of Environmental Concern: Properties, Distribu-

tion and Microbial Degradation Processes. *Chemosphere* **2011**, *83*, 1297−1306.

(6) Blondeau, M.; Coradin, T. Living Materials from Sol-Gel Chemistry: Current Challenges and Perspectives. *J. Mater. Chem.* **2012**, *22*, 22335−22343.

(7) Guo, L.; Jury, W. A.; Wagenet, R. J.; Flury, M. Dependence of Pesticide Degradation on Sorption: Nonequilibrium Model and Application to Soil Reactors. *J. Contam. Hydrol.* **2000**, *43*, 45−62.

(8) Guerin, W. F.; Boyd, S. A. Bioavailability of Naphthalene Associated with Natural and Synthetic Sorbents. *Water Res.* **1997**, *31*, 1504−1512.

(9) Smith, S. C.; Ainsworth, C. C.; Traina, S.; Hicks, R. J. The Effect of Sorption on the Biodegradation of Quinoline. *Soil Sci. Soc. Am. J.* **1992**, *56*, 737−746.

(10) Sievers, M., Advances Oxidation Processes. In *Treatise on Water Science*; Elsevier: Amsterdam, 2011; Vol. *4*, pp 377−408.

(11) Tada, H.; Jin, Q.; Iwaszuk, A.; Nolan, M. Molecular-Scale Transition Metal Oxide Nanocluster Surface-Modified Titanium Dioxide as Solar-Activated Environmental Catalysts. *J. Phys. Chem. C* **2014**, *118*, 12077−12086.

(12) Jin, Q.; Fujishima, M.; Iwaszuk, A.; Nolan, M.; Tada, H. Loading Effect in Copper(II) Oxide Cluster-Surface-Modified Titanium(IV) Oxide on Visible- and UV-Light Activities. *J. Phys. Chem. C* **2013**, *117*, 23848−23857.

(13) Pelaez, M.; Nolan, N. T.; Pillai, S. C.; Seery, M. K.; Falaras, P.; Kontos, A. G.; Dunlop, P. S. M.; Hamilton, J. W. J.; Byrne, J. A.; O'Shea, K.; Entezari, M. H.; Dionysiou, D. D. A Review on the Visible Light Active Titanium Dioxide Photocatalysts for Environmental Applications. *Appl. Catal., B* **2012**, *125*, 331−349.

(14) Finkelstein-Shapiro, D.; Hurst Petrosko, S.; Dimitrijevic, N. M.; Gosztola, D.; Gray, K. A.; Rajh, T.; Tarakeshwar, P.; Mujica, V. CO_2 Preactivation in Photoinduced Reduction Via Surface Functionalization of TiO_2 Nanoparticles. *J. Phys. Chem. Lett.* **2013**, *4*, 475−479.

(15) Gionco, C.; Paganini, M. C.; Giamello, E.; Burgess, R.; Di Valentin, C.; Pacchioni, G. Cerium-Doped Zirconium Dioxide, a Visible-Light-Sensitive Photoactive Material of Third Generation. *J. Phys. Chem. Lett.* **2014**, *5*, 447−451.

(16) Sannino, F.; Pirozzi, D.; Vitiello, G.; D'errico, G.; Aronne, A.; Fanelli, E.; Pernice, P. Oxidative Degradation of Phenanthrene in the Absence of Light Irradiation by Hybrid ZrO_2-Acetylacetonate Gel-Derived Catalyst. *Appl. Catal., B* **2014**, *101*, 156−157.

(17) Sannino, F.; Pirozzi, D.; Aronne, A.; Fanelli, E.; Spaccini, R.; Yousuf, A.; Pernice, P. Remediation of Waters Contaminated with MCPA by the Yeasts *Lipomyces starkeyi* Entrapped in a Sol−Gel Zirconia Matrix. *Environ. Sci. Technol.* **2010**, *44*, 9476−9481.

(18) Aronne, A.; Sannino, F.; Bonavolontà, S. R.; Fanelli, E.; Mingione, A.; Pernice, P.; Spaccini, R.; Pirozzi, D. Use of a New Hybrid Sol−Gel Zirconia Matrix in the Removal of the Herbicide MCPA: a Sorption/Degradation Process. *Environ. Sci. Technol.* **2012**, *46*, 1755−1763.

(19) Ozacar, M.; Sengil, I. A. A Two Stage Batch Adsorber Design for Methylene Blue Removal to Minimize Contact Time. *J. Environ. Manage.* **2006**, *80*, 372−379.

(20) Klepper, K. B.; Nilsen, O.; Hansen, P.-A.; Fjellvag, H. Atomic Layer Deposition of Organic−Inorganic Hybrid Materials Based on Saturated Linear Carboxylic Acids. *Dalton Trans.* **2011**, *40*, 4636−4646.

(21) Esposito, S.; Turco, M.; Bagnasco, G.; Cammarano, C.; Pernice, P.; Aronne, A. Highly Dispersed Sol−Gel Synthesized Cu−ZrO_2 Materials as Catalysts for Oxidative Steam Reforming of Methanol. *Appl. Catal., A* **2010**, *372*, 48−57.

(22) Aronne, A.; Vladimir, N.; Champagnon, S. B.; Fanelli, E.; Califano, V.; Usmanova, L. Z.; Pernice, P. The Origin of Nanostructuring in Potassium Niobiosilicate Glasses by Raman and FTIR Spectroscopy. *J. Non-Cryst. Solids* **2005**, *351*, 3610−3618.

(23) Costa, C.; Maia, S.; Silva, P.; Garrido, J.; Borges, F.; Garrido, E. M. Photostabilization of Phenoxyacetic Acid Herbicides MCPA and Mecoprop by Hydroxypropyl-*β*-cyclodextrin. *Int. J. Photoenergy* **2013**, http://dx.doi.org/10.1155/2013/542783.

(24) Vione, D.; Khanra, S.; Das, R.; Minero, C.; Maurino, V.; Brigante, M.; Mailhot, G. Effect of Dissolved Organic Compounds on the Photodegradation of the Herbicide MCPA in Aqueous Solution. *Water Res.* **2010**, *44*, 6053−6062.

(25) Burrows, H. D.; Canle, M.; Santaballa, J. A.; Steenkenc, S. Reaction Pathways and Mechanisms of Photodegradation of Pesticides. *J. Photochem. Photobiol., B* **2002**, *67*, 71−108.

(26) Önneby, K.; Håkansson, S.; Pizzul, L.; Stenström, J. Reduced Leaching of the Herbicide MCPA after Bioaugmentation with a Formulated and Stored Sphingobium sp. *Biodegradation* **2014**, *25*, 291−300.

(27) Bælum, J.; Henriksen, T.; Hansen, H. C. B.; Jacobsen, C. S. Degradation of 4-Chloro-2-Methylphenoxyacetic Acid in Top- and Subsoil Is Quantitatively Linked to the Class III *tfdA* Gene. *Appl. Environ. Microbiol.* **2006**, *72*, 1476−1486.

(28) Ranjit, P. J.; Palanivelu, K.; Lee, C. S. Degradation of 2,4-Dichlorophenol in Aqueous Solution by Sono-Fenton Method. *Korean J. Chem. Eng.* **2008**, *25*, 112−117.

(29) Gurol, M. D.; Vatistas, R. Oxidation of Phenolic Compounds by Ozone and Ozone+UV Radiation: a Comparative Study. *Water Res.* **1987**, *21*, 895−900.

(30) Li, X.-Y.; Cui, Y.-H.; Feng, Y.-J.; Xie, Z.-M.; Gu, J.-D. Reaction Pathways and Mechanisms of the Electrochemical Degradation of Phenol on Different Electrodes. *Water Res.* **2005**, *39*, 1972−1981.

(31) Ugurlu, M.; Karaoglu, M. H. TiO_2 Supported on Sepiolite: Preparation, Structural and Thermal Characterization and Catalytic Behaviour in Photocatalytic Treatment of Phenol and Lignin from Olive Mill Wastewater. *Chem. Eng. J.* **2011**, *166*, 859−867.

(32) Boye, B.; Dieng, M. M.; Brillas, E. Degradation of Herbicide 4-Chlorophenoxyacetic Acid by Advanced Electrochemical Oxidation Methods. *Environ. Sci. Technol.* **2002**, *36*, 3030−3035.

(33) Li Puma, G.; Toepfer, B.; Gora, A. Photocatalytic Oxidation of Multicomponent Systems of Herbicides: Scale-Up of Laboratory Kinetics Rate Data to Plant Scale. *Catal. Today* **2007**, *124*, 124−132.